Title	Deterministic and reliability assessment of basal heave stability for braced excavations with jet grout base slab
Author(s)	Goh, Anthony Teck Chee
Citation	Goh, A. T. C. (2017). Deterministic and reliability assessment of basal heave stability for braced excavations with jet grout base slab. Engineering Geology, 218, 63-69.
Date	2017
URL	http://hdl.handle.net/10220/44139
Rights	© 2017 Elsevier B.V. This is the author created version of a work that has been peer reviewed and accepted for publication by Engineering Geology, Elsevier B.V. It incorporates referee's comments but changes resulting from the publishing process, such as copyediting, structural formatting, may not be reflected in this document. The published version is available at: [http://dx.doi.org/10.1016/j.enggeo.2016.12.017].

Deterministic and reliability assessment of basal heave stability for braced excavations with jet grout base slab

A. T. C. Goh[1]

Abstract: For braced excavations in deep deposits of soft clays, it is common to construct a jet grout slab (JGP) beneath the excavation in order to restrain the wall deformation, reduce the forces acting on the struts and to increase the basal heave factor of safety. In this paper, finite element analyses were carried out to assess the basal heave factor of safety for excavations in soft clays supported by JGP. The finite element analyses indicate that the interface friction between the jet grout slab and the wall is a key component contributing to the resistance of the excavation system to basal heave failure. Comparison of the factor of safety from the finite element analyses with limit equilibrium predictions based on the slip circle method and the modified Terzaghi method were then performed. Since the conventional factor of safety approach does not explicitly reflect the uncertainties of the soil and JGP properties, and the excavation geometry on the excavation system performance, a series of reliability analyses were also carried out to assess the basal heave factor of safety for excavations supported by JGP. The provided spreadsheet template can be used to estimate the probability of basal heave failure for deep excavations supported by jet grout slabs.

KEY WORDS: basal heave; braced excavation; clay; factor of safety; jet grout pile; structural reliability.

[1]*Associate Professor, School of Civil & Environmental Engrg., Nanyang Technological University, Nanyang Avenue, Singapore 639798. E-mail: ctcgoh@ntu.edu.sg*

1. Introduction

Deep excavations in soft clays often result in excessive wall and ground movements which may cause damage to adjacent buildings and utilities. These movements can still be significant even with the use of stiff retaining walls systems such as diaphragm walls and secant bored piles and multiple levels of struts. One possible solution to minimize movements is to use concrete cross walls or buttress walls (Ou et al. 2006). Another possible solution is to use a ground improvement technique known as jet grouting prior to excavation (Wen 2005; Ou 2006). The jet grouting process produces a series of short overlapping grout columns to produce a "continuous" base slab (commonly termed as jet grout pile or JGP) below the final excavation level that spans across the entire excavation (Gaba 1990; Hsieh et al. 2003; Ho and Hu 2006). Typically, the JGP thickness ranges from 2 m to 4 m. In one particular large excavation (approximately 90 m wide and 240 m long) in Singapore, a 9 m thick JGP slab was used (Wong and Poh 2000). Generally, the JGP is designed to prevent basal heave instability (Shirlaw 2003), restrain the wall deformations and provide lateral support to reduce the forces acting on the struts. For example, the study by Hsieh et al. (2003) indicated reduction in the wall deformation by as much as 40% with the installation of a jet grout slab.

The focus of this paper is on the assessment of basal heave instability for deep excavations in clay with JGP. Comparative deterministic calculations of the basal heave factor of safety have been performed using limit equilibrium methods and nonlinear finite element analyses. Since the conventional factor of safety approach does not explicitly reflect the uncertainties of the soil and JGP properties, and the excavation geometry on the excavation system performance, it is demonstrated in this paper that a reliability based approach in a spreadsheet environment can be used to assess the probability of basal heave failure. Example applications of the use of probabilistic approaches in the design of braced excavations include

Goh and Kulhawy (2005), Park et al. (2007), Wu et al. (2010) and Luo et al. (2012).

2. Limit Equilibrium Method

The Terzaghi (1943), Bjerrum and Eide (1956) and Eide et al. (1972) methods which are based on bearing capacity theory are commonly used to assess basal heave stability for conventional excavations in clays. Another method that is commonly adopted in Japan and Taiwan is the slip circle method which involves taking moments about the lowest strut level (JSA 1988; Hsieh et al. 2008; Luo et al. 2012). The slip circle method has also been applied for excavations with a JGP at the base by incorporating the undrained shear strength of the JGP. In the slip circle method, the basal heave factor of safety FS_{slip} is assessed by taking moments about the lowest strut level (Fig. 1)

$$FS_{slip} = \frac{M_r}{M_d} = \frac{R\int_0^{\theta+\pi/2} c_u d\omega + R\int_0^{\beta} c_{uJ} d\omega}{W(R/2) + q(R^2/2)} \quad (1)$$

where M_r = resisting moment; M_d = driving moment; R = radius of the failure slip circle; W = weight of the soil mass behind the wall and above the excavation level; q = surcharge pressure; H = excavation depth; D = wall penetration depth; B = excavation width; c_u = clay undrained shear strength; c_{uJ} = JGP undrained shear strength; θ and β = angles shown in Fig. 1.

Fig. 1. Slip circle method for basal heave stability of jet grout pile

For comparison, another limit equilibrium method called the modified Terzaghi method (Wong and Goh 2002; Goh et al. 2008) is used to assess the basal heave factor of safety for excavations involving a JGP layer. In this method, the effects of the JGP is considered by

assuming that failure occurs beneath the base of the JGP and is partially resisted by the interior JGP-wall adhesion $f_s = \alpha_J c_{uJ}$ (Eide et al. 1972), as illustrated in Fig. 2, in which α_J is the JGP-wall adhesion factor. The factor of safety FS_{mT} can be expressed as:

$$FS_{mT} = \frac{5.7c_{ub}B_1 + c_{uh}H + c_{ud}D + f_sD}{(\gamma H + q)B_1} \quad (2)$$

where $B_1 = (B/\sqrt{2})$. The value of 5.7 in the first term of the numerator of Eq. (2) corresponds to the bearing capacity factor N_c for a rough footing. As illustrated in Fig 2, c_{uh} is the undrained shear strength of the clay from the ground surface to the final depth of excavation H, c_{ud} is the undrained shear strength of the clay from depth H to the tip of the wall, and c_{ub} is the undrained shear strength of the clay below the final excavation level.

Fig. 2. Modified Terzaghi method for basal heave stability of jet grout pile

3. Finite Element Analyses

In this study, extensive plane strain finite element analyses were carried out to assess the basal heave factor of safety for excavations with JGP. The parametric study was performed using the finite element software Plaxis (Brinkgreve et al. 2011). A typical very refined mesh comprising 3,226 elements and 26,409 nodes is shown in Fig. 3. Because of symmetry, only half the cross-section was considered. The soil was modeled by 15-noded triangular elements. The wall structural elements were assumed to be linear elastic and were modeled by 5-noded beam elements. The interface elements that model the slippage between the soil and the wall consist of 10-noded joint elements. The shear response of the interface element is controlled by an elastic–perfectly plastic Coulomb shear strength criterion. The struts (not shown in Fig.

3) were modeled by linear elastic 3-noded bar elements. The nodes along the side boundaries of the mesh were constrained from displacing horizontally while the nodes along the bottom boundary were constrained from moving horizontally and vertically. The right vertical boundary extends far from the excavation (~5B) to minimize the effects of the boundary restraints.

The Hardening Soil (HS) constitutive relationship was used to model the undrained behavior of the clay and the JGP. The HS model is an elastic-plastic soil model based on the classical plasticity theory (Schanz et al. 1999; Brinkgreve et al. 2011) for simulating the behavior of soils. The model involves frictional hardening characteristics to model plastic shear strain in deviatoric loading, and cap hardening to model plastic volumetric strain in primary compression. Failure is defined by the Mohr Coulomb failure criterion. The main input parameters are E_{50}^{ref}, a reference secant modulus corresponding to the reference confining pressure p_{ref}, a power m for stress-dependent stiffness formulation, friction angle ϕ, cohesion c, failure ratio R_f, E_{ur}^{ref} the reference stiffness modulus for unloading and reloading corresponding to p_{ref}, and υ_{ur} the unloading and reloading Poisson's ratio. This model has been used successfully for analyses of deep excavations by a number of researchers in Singapore (Teo and Wong 2012) and elsewhere (Finno et al. 2007; Bryson and Zapata-Medina 2012; Surarak et al. 2012). For this study, only cases with a homogeneous clay layer with constant undrained shear strength c_u were considered. The soil is assumed to be subjected to undrained shearing during excavation. Only clays with isotropic c_u are considered. The depth to the hard stratum is assumed to be large. The properties of the JGP (see Table 1) are based on common design values used in Singapore (Ho and Hu 2006). In addition, it is assumed that the wall has enough capacity not to fail under the action of deep-seated soil movements.

A total of 55 different cases were analyzed. The range of geometrical properties of the excavation that were analyzed, and the assumed structural, JGP and soil properties are shown in Table 1.

Fig. 3. Typical finite element mesh (struts not shown)

Table 1. Summary of JGP, soil, structural and geometrical properties.

The construction sequence comprised the following steps: (1) the wall and JGP are installed ("wished into place") without any disturbance in the surrounding soil; (2) the soil is excavated uniformly in 2 m intervals, and struts are installed until the final depth H is reached. The stability of the excavation was then determined using the shear strength reduction technique. This technique has been used by various authors including Griffiths and Lane (1999), Hammah et al. (2007), Park et al. (2007); Zhang and Goh (2012) and Do et al. (2013). The method is now available in many commercial finite element and finite difference programs.

The procedure essentially involves repeated analyses by progressively reducing the shear strength properties of the soil and the JGP until collapse occurs. By reducing the shear strength by a factor F the shear strength equation becomes:

$$\frac{\tau}{F} = \frac{c}{F} + \sigma_n \frac{\tan\phi}{F} \tag{3}$$

where τ is the shear strength, σ_n is the normal stress, and $c^* = c/F$ and $\phi^* = \arctan(\tan\phi/F)$ are the modified Mohr-Coulomb shear strength parameters. Systematic increments of F are

performed until the finite element model does not converge to a solution (i.e. failure occurs). The critical strength reduction value which corresponds to non-convergence is taken to be the basal heave factor of safety FS_{FE}.

4. Finite Element Results

For brevity, only some general trends of the finite element analyses are highlighted. The influence of the width of the excavation B are shown in Figs. 4 and 5 for two different excavation depths H = 16 m and H = 24 m, respectively. The basal heave factor of safety FS_{FE} decreases with the increase of the excavation width. Comparing the factor of safety with and without the JGP, the increase in FS_{FE} with the JGP is more significant for $B \leq 20$ m. For example, for the case with B = 20 m and H = 16 m, the installation of a 4 m thick JGP increased the basal heave factor of safety by 31% compared with a 16% increase for B = 30 m.

Fig. 6 shows the influence of the JGP-wall adhesion factor α_J on the factor of safety. The factor of safety reduces significantly for $\alpha_J \leq 0.67$. For example, for the case with B = 20 m and H = 16 m, the installation of the JGP increased the FS_{FE} by 31% for $\alpha_J = 1$, compared with an increase of 17% for $\alpha_J = 0.5$. The results highlight that the interface friction between the jet grout slab and the wall is a key component of the resistance of the excavation system to basal heave failure. As expected, the factor of safety increases with increased thickness of the JGP as shown in Fig. 7.

Fig. 4. Effects of excavation width B on FS_{FE} (H = 16 m and c_u = 50 kPa)

Fig. 5. Effects of excavation width B on FS_{FE} (H = 24 m and c_u = 80 kPa)

Fig. 6. Effects of JGP-wall interface adhesion factor on FS_{FE} (B = 20 m, H = 16 m, D = 4 m and c_u = 50 kPa)

Fig. 7. Effects of JGP thickness on FS_{FE} (B = 20 m, H = 16 m, and c_u = 50 kPa)

Comparison of the FS_{FE} values with the predictions based on the slip circle method (FS_{slip}) and the modified Terzaghi method (FS_{mT}) are shown in Fig. 8. Generally, there is more scatter in the FS_{slip} predictions using the slip circle method compared with the predictions using FS_{mT}. The modified Terzaghi method generally predicts reasonable values of the basal heave factor of safety FS_{mT} compared with FS_{FE}. In this study, only clays with constant c_u were considered. In the previous study by Wong & Goh (2002), it was found that for clays with c_u increasing linearly with depth, both the Terzaghi method and modified Terzaghi method were found to give good estimations of the factor of safety (compared with the finite element results) if the average c_u values were used. For example, the c_{uh} value is taken as the average c_u from the ground surface to the depth H, and the c_{ub} value is taken as the average cu from depth H to depth (H + B_1). The same approach was found to work in applying the modified Terzaghi equation (Eq. 2) to cases of JGP stabilized soil. For brevity, the results have been omitted in this paper.

Fig. 8. Comparison of FS_{FE} versus FS predicted using slip circle (FS_{slip}) and modified Terzaghi (FS_{mT}) methods

5. Reliability Analyses

Since the deterministic factor of safety approach outlined in the previous section does not explicitly reflect the uncertainties of the soil and JGP properties, and the excavation geometry on the excavation system performance, a reliability based approach is proposed in this section to assess the probability of basal heave failure.

In the conventional deterministic evaluation of geotechnical stability, the factor of safety is defined as the ratio of the resistance *R* to the load (stress) *S*. In the reliability approach, the boundary separating the safe and failure domain is the limit state surface (boundary) defined as:

$$G(\mathbf{x}) = R - S = 0 \qquad (4)$$

where **x** denotes the vector of the random variables. Mathematically, $R > S$ or $G(\mathbf{x}) > 0$ would denote a 'safe' domain, and $R < S$ or $G(\mathbf{x}) < 0$ would denote a 'failure' domain. The calculation of the probability of failure P_f involves the integration of the probability density function (pdf) over the failure domain.

One method to quantify the probability of failure is to carry out Monte Carlo simulations using random variables with specified joint probability distributions to represent the geotechnical uncertainties and to perform a large number of deterministic analyses. Clear expositions of the reliability approach are found in various publications (Ang and Tang 1984; Melchers 1987; Baecher and Christian 2003). A well-developed approximate alternative is to use the First-Order Reliability Method (FORM) proposed by Hasofer and Lind (1974). Its popularity results from the mathematical simplicity, since only second moment information

(mean and standard deviation) on the random variables is required to calculate the reliability index β. Mathematically, β can be computed as

$$\beta = \min_{x \in F} \sqrt{\left(\frac{x_i - \mu_i}{\sigma_i}\right)^T [R]^{-1} \left(\frac{x_i - \mu_i}{\sigma_i}\right)} \quad (5)$$

in which x_i is the set of n random variables, μ_i is the set of mean values, R is the correlation matrix and F is the failure region. The minimization in Eq. (5) is performed over F corresponding to the region G(**x**) = 0. Low (2005) had shown that a spreadsheet environment can be used to perform the minimization and determine β. The probability of failure is inferred from the reliability index as

$$P_f \approx \Phi(-\beta) \quad (6)$$

in which Φ(-β) is the value of the cumulative probability. Examples of the use of reliability to assess basal heave stability in conventional excavations can be found in Park et al. (2007), Goh et al. (2008), and Wu et al. (2010).

In this paper, the spreadsheet solution implementing the first order reliability method FORM for basal heave stability using the modified Terzaghi method to determine the factor of safety FS (Goh et al. 2008) has been adopted taking into consideration the JGP-wall interface adhesion f_s. In a previous study (Goh et al. 2008), in which basal heave reliability analyses were considered for Terzaghi's method, modified Terzaghi's method, Bjerrum & Eide method, and Eide's method, the main properties influencing the probability of failure were found to be the soil unit weight and soil undrained shear strength and their COV. The

uncertainties (COV) in the geometrical properties of the excavation system were found to have minimal influence on the probability of failure. As an illustration, in this paper, only the uncertainties in the surcharge, soil and JGP parameters, and H and D were considered. Fig. 9 shows an example setup of the spreadsheet for evaluating the reliability index for the modified Terzaghi expression in Eq. (2). There are eight lognormally distributed and uncorrelated variables: c_{ub}, c_{uh}, q, γ, H, c_{ud}, f_s and D. The width of the excavation B is assumed to be constant. The uncertainties in the parameters H and D could arise from construction deviations in the actual excavation depth and depth of wall penetration, respectively. Detailed explanations of the spreadsheet setup can be found in Goh et al. (2008).

Initially, the **x** values of the variables (cells C5 to C12) are set to the mean values (cells D6 to D12). For evaluating the probability of failure, the design safety level FS_{limit} (cell O29) is set to unity. The reliability index β and the probability of failure P_f are calculated in cell D32 and cell E32, respectively. The Solver spreadsheet function is invoked to minimize β by changing the **x** values (cells C5 to C12) subject to $G(\mathbf{x}) = FS - FS_{limit} = 0$ (cell O32).

Fig. 9. Spreadsheet setup for reliability analysis

Since a comparison on the factor of safety based on the modified Terzaghi method (in section 4) was found to be in good agreement with the finite element results, it has been assumed that the model error (imperfection of the prediction model) is minimal compared with the other random variables. If the model error is significant, one or more random variable correction factors can be incorporated into the limit state surface equation as described in Ang and Tang (1984). In this paper, the uncertainties (inherent variability) of the soil and JGP are limited to the coefficient of variation (COV: standard deviation divided by the mean) of the

geotechnical properties. As there is only sparse published data on the spatial variability (and also inherent variability) of the JGP geotechnical properties, the spatial variability (Vanmarcke, 1977) is not addressed in this paper.

This section presents the results of analyses to assess the probability of failure P_f ($FS \leq 1$) for excavations in clays with FS_{mean} values ranging from 1.2 to 1.7, where FS_{mean} is the factor of safety computed using the mean values of the parameters. In all the analyses, the mean and COV of the surcharge adjacent to the excavation q and the unit weight of the clay γ are assumed to be unchanged ($mean_q$ = 10 kPa/m, COV_q = 0.2; $mean_\gamma$ = 16 kN/m^3, COV_γ = 0.15). Based on the database by Phoon and Kulhawy (1999) the inherent variability of the undrained shear strength of clay is 0.3. Hence, for the majority of the analyses, the COVs of the soil undrained shear strength (for simplicity, the term COV_{cu} is used) was assumed to be 0.3. Some analyses were also carried out for COV_{cu} = 0.2.

The results of a series of analyses for FS_{mean} values ranging from 1.2 to 1.7 for COV_{cu} = 0.3 and COV_{cu} = 0.2 are shown in Table 2 and Fig. 10. The FS_{mean} is calculated based on Eq. (2). The results highlight the significant influence of the COV_{fs} of the JGP-wall adhesion on the probability of failure P_f as the COV of f_s is increased from 0.1 to 0.6. As expected, for a given FS_{mean}, the probability of failure P_f increases as the COV_{fs} increases. For example, for FS_{mean} = 1.5, P_f increased 41% as the COV_{fs} increases from 0.1 to 0.4. For FS_{mean} = 1.5 and COV_{fs} = 0.6, the probability of basal heave failure is still fairly high (9.1%). The same trends are observed for cases with COV_{cu} = 0.2. The results highlight the influence of the COV_{cu} on the probability of failure. For example, with a reduction in the COV_{cu} from 0.3 to 0.2, for FS_{mean} = 1.5 and COV_{fs} = 0.6, the probability of basal heave failure is reduced from 9.1% to 4.6%. The above results show that the same factor of safety can have vastly different levels of risk

depending on the degree of uncertainty of COV_{cu} and COV_{fs}. The proposed reliability approach provides a systematic method for evaluating the influences of the uncertainties in the various parameters affecting FS_{mean} and to assist design engineers assess the acceptable level of risk.

Table 2. Probability of failure for $COV_{cu} = 0.2$ and $COV_{cu} = 0.3$

Fig. 10. Plot of P_f for various COV_{cu} and COV_{fs}

6. Summary

Finite element analyses were carried out to assess the basal heave factor of safety for excavations in soft clays supported by JGP. A total of 55 different cases with different geometrical properties of the excavation, JGP and soil properties were considered. The basal heave factor of safety FS_{FE} was found to decrease with the increase of the excavation width. Comparing the factor of safety with and without the JGP, the increase in FS_{FE} with the JGP is more significant for $B \leq 20$ m. The finite element analyses also highlight that the interface friction between the jet grout slab and the wall is a key component of the resistance of the excavation system to basal heave failure.

Comparison of the FS_{FE} values with the predictions based on the slip circle method and the modified Terzaghi method was also performed. Generally, there is more scatter in the FS_{slip} predictions using the slip circle method compared with the predictions using FS_{mT}. The modified Terzaghi method generally predicts reasonable values of the basal heave factor of safety FS_{mT} compared with FS_{FE}.

A series of reliability analyses were then carried out to assess the basal heave factor of safety for excavations supported by JGP. The results show that the same factor of safety can have vastly different levels of risk depending on the degree of uncertainty of the design parameters. For example, for FS_{mean} = 1.5 and COV_{cu} = 0.3, the P_f is approximately 5% for COV_{fs} = 0.1. The P_f increases to approximately 9% for COV_{fs} = 0.6. The provided spreadsheet template can be used to estimate the probability of basal heave failure for deep excavations supported by jet grout slabs. The reliability approach provides a systematic method for evaluating the influences of the uncertainties in the various parameters affecting FS_{mean} and can be used to assist design engineers assess the acceptable level of risk. In this paper, the uncertainties (inherent variability) of the soil and JGP are limited to the coefficient of variation of the geotechnical properties. As there is only sparse published data on the spatial variability of the JGP geotechnical properties, the spatial variability is not addressed in this paper.

References

Ang, A.H.S., Tang, W.H., 1984. Probability concepts in engineering planning and design. Vol. II - Decision, risk and reliability. John Wiley & Sons, New York.

Baecher, G.B., Christian, J.T., 2003. Reliability and statistics in geotechnical engineering. John Wiley & Sons, New York.

Bjerrum, L., Eide, O., 1956. Stability of strutted excavations in clay. Geotechnique. 6(1), 32-47.

Brinkgreve, L.B.J., Engin, E., Swolfs, W.M., 2011. Plaxis user manual, PLAXIS bv, Netherlands.

Bryson, L., Zapata-Medina, D., 2012. Method for estimating system stiffness for excavation support walls. J. Geotech. Geoenviron. Eng. ASCE 138 (9), 1104-1115.

Do, T., Ou, C. ., Lim, A., 2013. Evaluation of factors of safety against basal heave for deep excavations in soft clay using the finite-element method. J. Geotech. Geoenviron. Eng. ASCE 139 (12), 2125-2135.

Eide, O., Aas, G., Josang, T., 1972. Special applications of cast-in-place walls for tunnels in soft clay in Oslo. Pub. 91, Norwegian Geotechnical Institute, Oslo, 63-72.

Finno, R.J., Blackburn, J.T., Roboski, J. F., 2007. Three-dimensional effects for supported excavations in clay. J. Geotech. Geoenviron. Eng. ASCE 133 (1), 30-36.

Gaba, A.R., 1990. Jet grouting at Newton Station, Singapore. Proc. 10th Southeast Asian Geotech Conf., Taipei, Taiwan, SEAGC, 77-79.

Goh, A.T.C., Kulhawy, F.H., 2005. Reliability assessment of serviceability performance of braced retaining walls using a neural network approach. Int. J. Num. Analy. Meth. Geomech. 29 (6), 627-642.

Goh, A.T.C, Kulhawy, F.H., Wong, K.S., 2008. Reliability assessment of basal-heave stability for braced excavations in clay. J. Geotech. Geoenviron. Eng. ASCE 134 (2), 145-153.

Griffiths, D.V., Lane, P.A., 1999. Slope stability analysis by finite elements. Géotechnique 49 (3), 387-403.

Hammah, R.E., Yacoub, T., Curran, J.H., 2007. Serviceability-based slope factor of safety using the shear strength reduction (SSR) method. The Second Half Century of Rock Mechanics 11th Congress of the International Society for Rock Mechanics, Taylor & Francis, 1137-1140.

Hasofer, A.M., Lind, N.C., 1974. An exact and invariant first-order reliability format. J. Eng. Mech., ASCE 100 (1), 111-121.

Ho, C.E., Hu, S., 2006. Numerical analysis of jet grout elements for braced excavation in soft clay. Proc. ASCE GeoCongress 2006: Geotechnical Engineering in the Information Technology Age, Atlanta, Georgia. 1-6.

Hsieh. H.S., Wang, C.C., Ou, C.Y., 2003. Use of jet grouting to limit diaphragm wall displacement of a deep excavation. J. Geotech. Geoenviron. Eng. ASCE 129 (2), 146-157.

Hsieh. P.G., Ou, C.Y., Liu H.T., 2008. Basal heave analyses of excavations with consideration of anisotropic undrained strength of clay. Can. Geotech. J. 45, 788-799.

JSA, 1988. Guidelines of design and construction of deep excavations. Japanese Society of Architecture, Tokyo, Japan.

Low, B.K., 2005. Reliability-based design applied to retaining walls. Geotechnique 55 (1), 63-75.

Luo, Z., Atamturktur, S, Cai, Y, Juang, C.H., 2012. Reliability analysis of basal-heave in a braced excavation in a 2-D random field. Comp. Geot. 39, 27-37.

Melchers, R.E., 1987. Structural reliability: Analysis and prediction. Ellis Horwood Ltd., Chichester, England.

Ou, C.Y., 2006. Deep Excavation: Theory and Practice. Taylor & Francis Group, London.

Ou, C.Y., Lin, Y.L., Hsieh, P.G., 2006. Case record of an excavation with cross walls and buttress walls. Journal of GeoEng. 1 (2), 79-86.

Park, J.K., Blackburn, J.T., Gardoni, P., 2007 Reliability assessment of excavation systems considering both stability and serviceability performance. Georisk 1 (3), 123-141.

Phoon, K.K., Kulhawy, F.H., 1999. Characterization of geotechnical variability. Can. Geot. J. 36 (4), 612-624.

Schanz, T., Vermeer, P.A., Bonnier, P.G., 1999. The hardeing soil model -formulation and verification. Proc., Beyond 2000 in Computational Geotechnics-10 years PLAXIS, Balkema, Rotterdam, 281-296.

Shirlaw, J.N., 2003. Jet grouting soft clays for tunneling and deep excavations – design and construction issues. Proc. 3rd Int. Conf., Grouting and Grout Treatment, ASCE 1, 257-268.

Surarak, C., Likitlersuang, S., Wanatowski, D., Balasubramaniam, A., Oh, E., Guan, H., 2012. Stiffness and strength parameters for hardening soil model of soft and stiff Bangkok clays. Soils Found. 52 (4), 682–697

Terzaghi, K., 1943. Theoretical soil mechanics. John Wiley & Sons, New York.

Teo, P.L., Wong, K.S., 2012. Application of the Hardening Soil model in deep excavation analysis. The IES Journal Part A: Civil & Struct. Eng. 5 (3), 152-165.

Vanmarcke, E.H., 1977. Probabilistic modeling of soil profiles. J. Geotech. Eng. ASCE 103 (11), 1227-1246.

Wen, D., 2005. Use of jet grouting in deep excavations. In Ground improvement – case histories. Editors: B. Indraratna & J. Chu. Elsevier. 357-370.

Wong I.H., Poh, T.Y., 2000. Effects of jet grouting on adjacent ground and structures. J. Geotech. Geoenviron. Eng. ASCE 126 (3), 247-256.

Wong, K.S., Goh, A.T.C., 2002. Basal heave stability for wide excavations. Proc. 3rd Int. Symp. Geotech. Aspects of Underground Construction in Soft Ground, Toulouse, 699-704.

Wu, S.H., Ou, C.Y., Ching, J., Juang, C.H., 2012. Reliability-based design for basal heave stability of deep excavations in spatially varying soils, J. Geotech. Geoenviron. Eng. ASCE 138 (5), 594-603.

Zhang, W.G., Goh, A.T.C., 2012. Reliability assessment on ultimate and serviceability limit states and determination of critical factor of safety for underground rock caverns. Tunnel Underg. Space Technol. 32, 221–230.

LIST OF TABLES

LIST OF FIGURES

Table 1. Summary of JGP, soil, structural and geometrical properties

Parameter	**Range of values**
Geometrical, strut and wall properties	
Excavation width B (m)	10 – 60
Excavation depth H (m)	16 – 24
Depth of wall penetration D (m)	3 - 8
Thickness of JGP (m)	3 - 8
Wall stiffness EI (kNm^2/m)	4.032×10^6
Wall axial stiffness EA (kN/m)	3.36×10^7
Strut axial stiffness EA (kN)	2.0×10^6
Soil and JGP properties	
Soil unit weight γ (kN/m^3)	16
Soil undrained shear strength c_u (kPa)	30 - 80
Soil modulus ratio E_{50}^{ref}/c_u	300
Unloading and reloading stiffness E_{ur}^{ref}	$3\ E_{50}^{ref}$
Unloading and reloading Poisson's ratio υ_{ur}	0.2
Stress-dependent stiffness ratio m	0
Failure ratio R_f	0.9
JGP shear strength c_{uJ} (kPa)	300 - 500
JGP E_{50}^{ref} (MPa)	150
JGP-wall adhesion factor α_J	0.2 – 1.0

Table 2. Probability of failure for COV_{cu} = 0.2 and COV_{cu} = 0.3

	P_f (FS ≤ 1)							
	COV_{cu} = 0.2				**COV_{cu} = 0.3**			
	COV_{fs}				**COV_{fs}**			
FS_{mean}	0.1	0.2	0.3	0.4	0.1	0.2	0.3	0.4
1.2	0.179	0.191	0.229	0.273	0.243	0.254	0.287	0.326
1.4	0.044	0.049	0.067	0.089	0.089	0.096	0.118	0.144
1.5	0.020	0.023	0.033	0.046	0.051	0.056	0.072	0.091
1.6	0.009	0.010	0.015	0.022	0.029	0.032	0.043	0.055
1.7	0.004	0.004	0.007	0.011	0.016	0.018	0.025	0.033

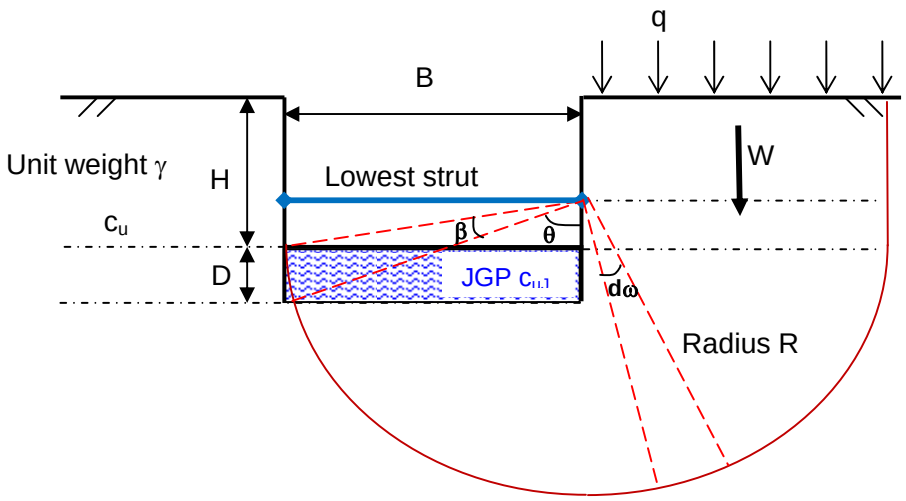

Fig. 1. Slip circle method for basal heave stability of excavation with jet grout pile.

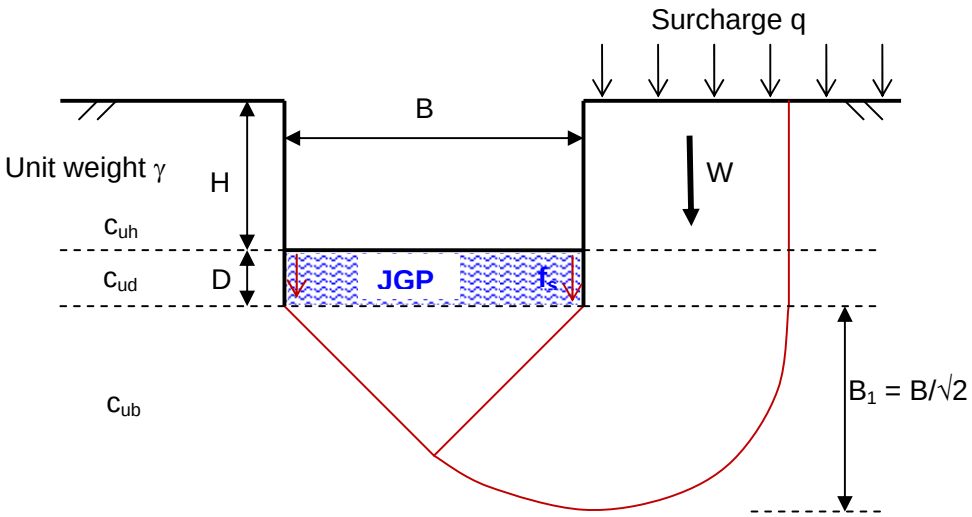

Fig. 2. Modified Terzaghi method for basal heave stability of excavation with jet grout pile

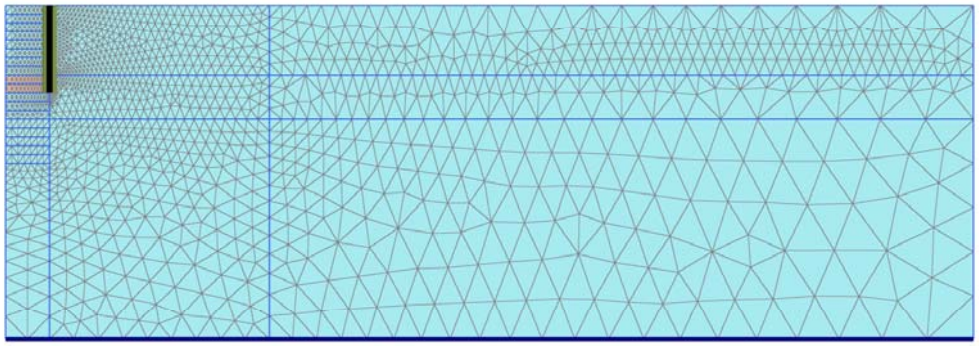

Fig. 3. Typical finite element mesh (struts not shown)

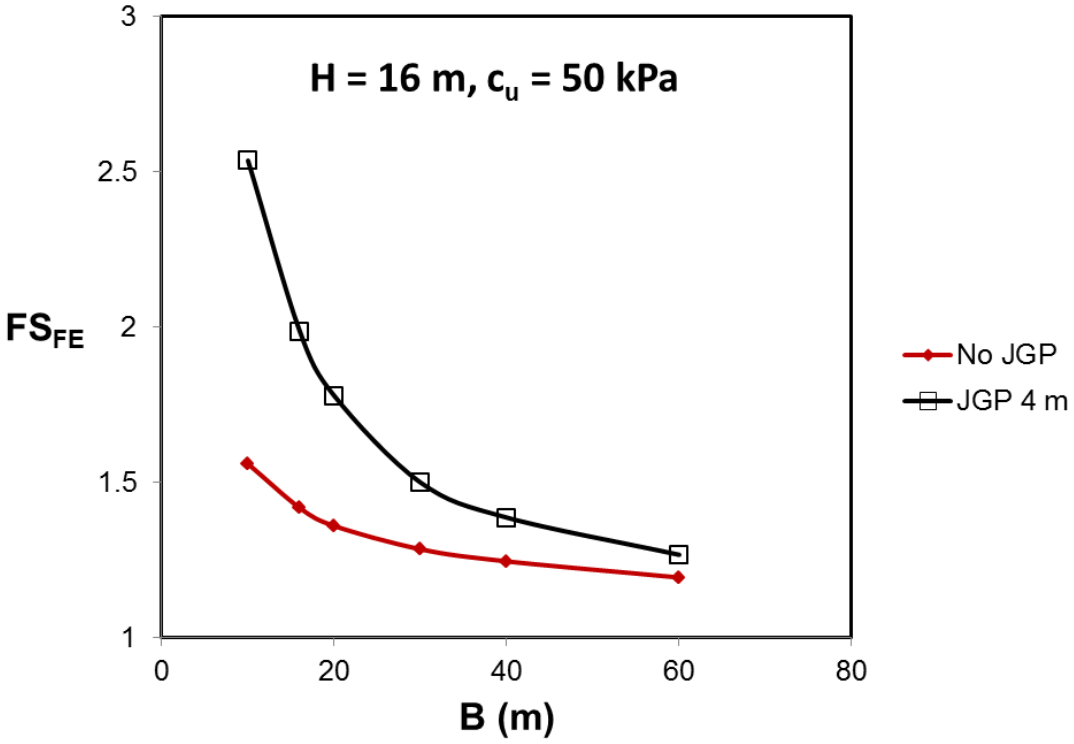

Fig. 4. Effects of excavation width B on FS_{FE} (H = 16 m and c_u = 50 kPa)

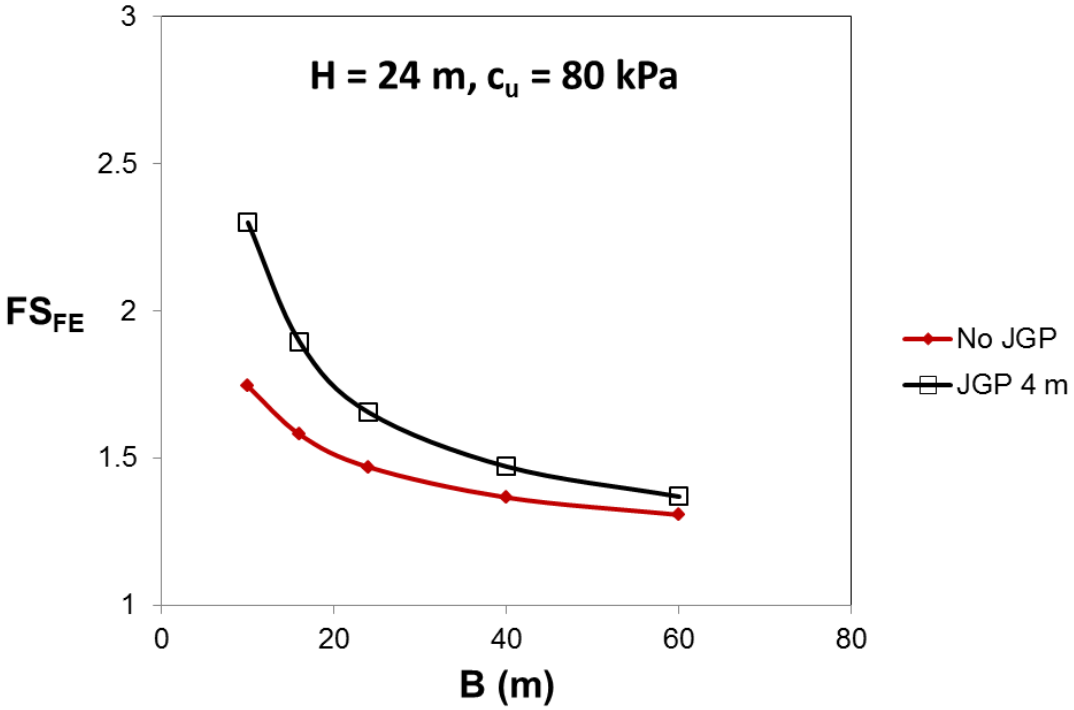

Fig. 5. Effects of excavation width B on FS_{FE} (excavation depth H = 24 m and c_u = 80 kPa)

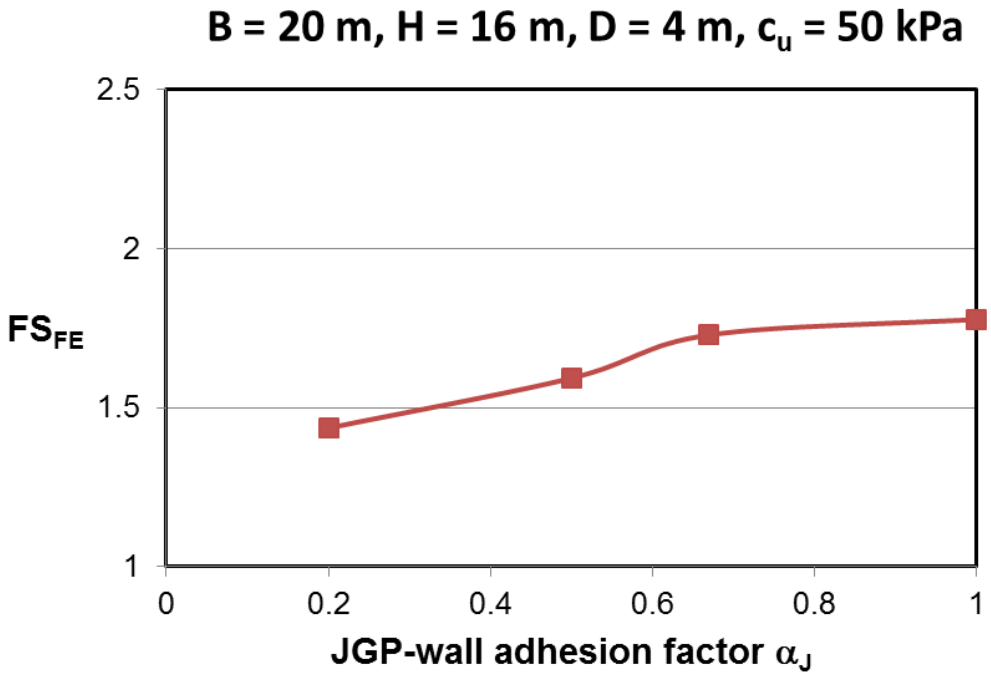

Fig. 6. Effects of JGP-wall interface adhesion factor on FS_{FE} (B = 20 m, H = 16 m, D = 4 m and c_u = 50 kPa)

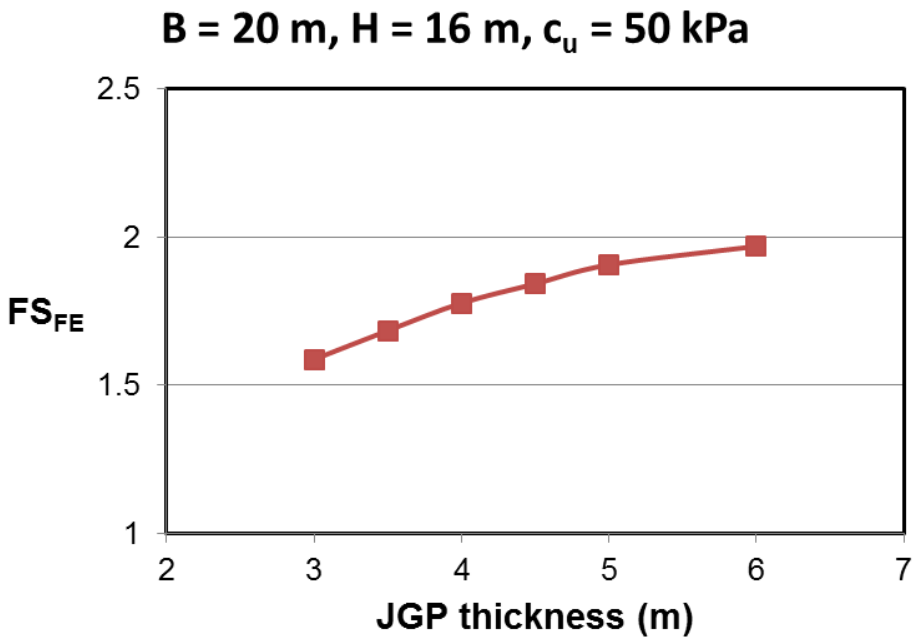

Fig. 7. Effects of JGP thickness on FS_{FE} (B = 20 m, H = 16 m, and c_u = 50 kPa)

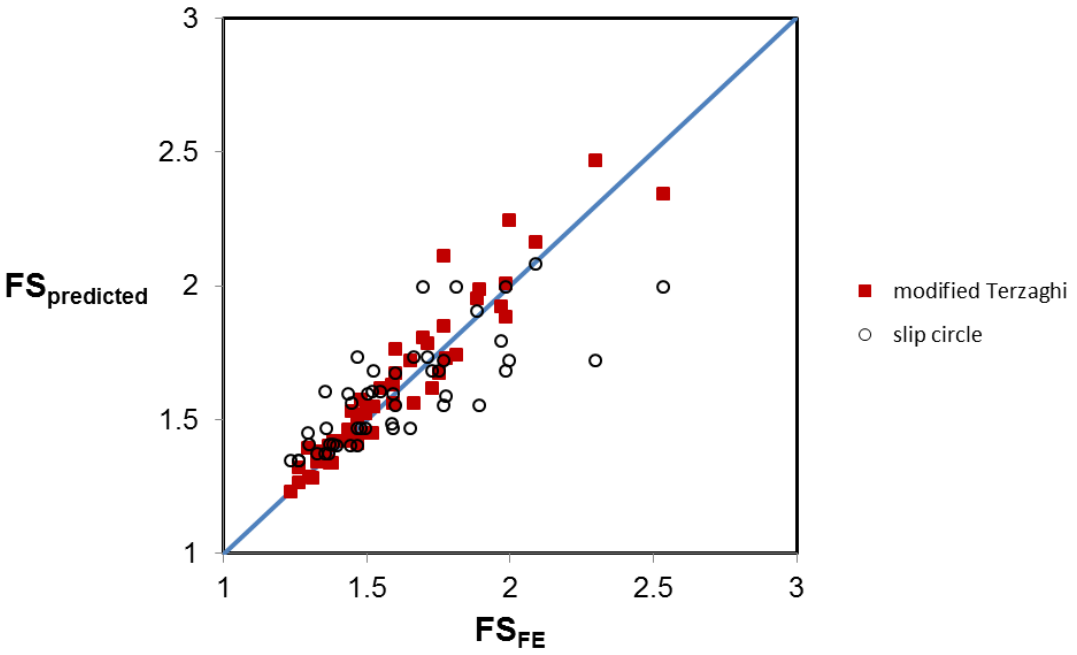

Fig. 8. Comparison of FS_{FE} versus FS predicted using slip circle (FS_{slip}) and modified Terzaghi (FS_{mT}) methods

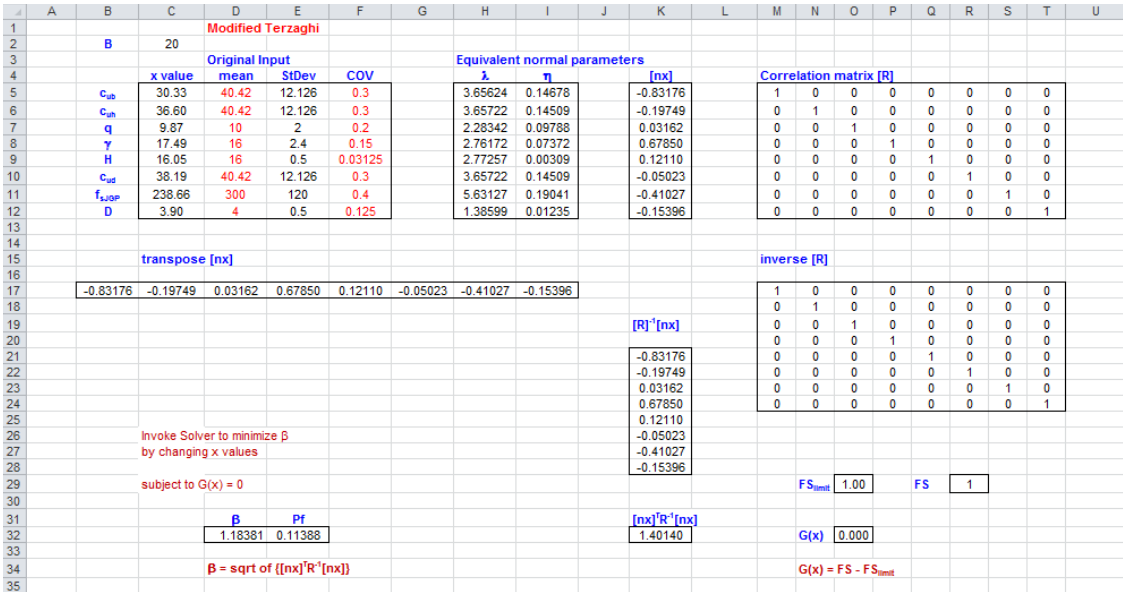

				Modified Terzaghi																
	B	20																		
			Original Input				Equivalent normal parameters					Correlation matrix [R]								
		x value	mean	StDev	COV		λ	η		[nx]										
	c_{ub}	30.33	40.42	12.126	0.3		3.65624	0.14678		-0.83176		1	0	0	0	0	0	0	0	
	c_{uh}	36.60	40.42	12.126	0.3		3.65722	0.14509		-0.19749		0	1	0	0	0	0	0	0	
	q	9.87	10	2	0.2		2.28342	0.09788		0.03162		0	0	1	0	0	0	0	0	
	γ	17.49	16	2.4	0.15		2.76172	0.07372		0.67850		0	0	0	1	0	0	0	0	
	H	16.05	16	0.5	0.03125		2.77257	0.00309		0.12110		0	0	0	0	1	0	0	0	
	c_{ud}	38.19	40.42	12.126	0.3		3.65722	0.14509		-0.05023		0	0	0	0	0	1	0	0	
	$f_{s/GP}$	238.66	300	120	0.4		5.63127	0.19041		-0.41027		0	0	0	0	0	0	1	0	
	D	3.90	4	0.5	0.125		1.38599	0.01235		-0.15396		0	0	0	0	0	0	0	1	
		transpose [nx]										inverse [R]								
	-0.83176	-0.19749	0.03162	0.67850	0.12110	-0.05023	-0.41027	-0.15396				1	0	0	0	0	0	0	0	
												0	1	0	0	0	0	0	0	
										$[R]^{-1}[nx]$		0	0	1	0	0	0	0	
												0	0	0	1	0	0	0	0	
										-0.83176		0	0	0	0	1	0	0	0	
										-0.19749		0	0	0	0	0	1	0	0	
										0.03162		0	0	0	0	0	0	1	0	
										0.67850		0	0	0	0	0	0	0	1	
										0.12110										
		Invoke Solver to minimize β								-0.05023										
		by changing x values								-0.41027										
										-0.15396										
		subject to G(x) = 0											FS_{limit}	1.00		FS	1			
			β	Pf						$[nx]^T R^{-1}[nx]$			G(x)	0.000						
			1.18381	0.11388						1.40140										
		β = sqrt of $([nx]^T R^{-1}[nx])$											G(x) = FS - FS_{limit}							

Fig. 9. Spreadsheet setup for reliability analysis

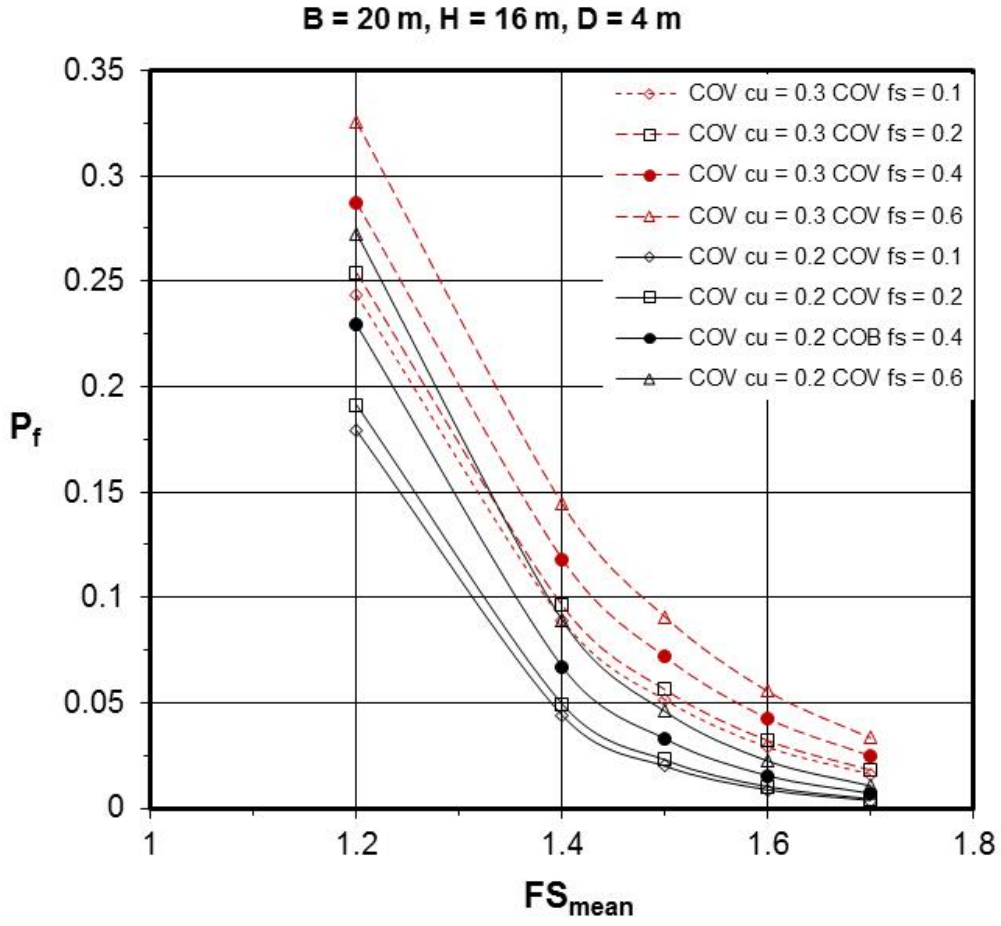

Fig. 10. Plot of probability of failure P_f for various COV_{cu} and COV_{fs}